Phase Diagram of Pentacene Growth on Au(110)

Luca Floreano,*,† Albano Cossaro,† Dean Cvetko,†,‡,§ Gregor Bavdek,†,§ and Alberto Morgante†,§,||

CNR−INFM Laboratorio Nazionale TASC, Basovizza SS-14, Km 163.5, I-34012 Trieste, Italy

Received: September 28, 2005; In Final Form: January 24, 2006

We studied the growth of pentacene ($C_{22}H_{14}$) on the Au(110) surface by means of He atom scattering and Synchrotron X-ray photoemission. We found that two-dimensional commensurate growth only occurs in the monolayer range for a substrate temperature, T_s, higher than ∼370 K. Larger amounts of deposited molecules forms three-dimensional uncorrelated clusters on the wetting layer. The desorption of second layer molecules occurs at $T_s \geq 420$ K. The highest coverage ordered phase displays a (6×8) symmetry and corresponds to the saturation coverage at $T_s = 420$ K. The (3×6) symmetry phase, recently reported for a multilayer planar film [Ph. Guaino, et al. *Appl. Phys. Lett.* **2004**, *85*, 2777], is only found at a coverage slightly lower than the (6×8) one. The (3×6) phase corresponds to the saturation coverage of the first layer at $T_s = 470$ K.

1. Introduction

π-conjugated molecules are a cost-effective solution to the fabrication of large area electronic devices.[1] As a drawback, their charge transport properties deteriorate strongly with increasing density of structural defects and grain boundaries that, unlike in semiconductor devices, are commonly present in organic films.[2] In fact, orientationally ordered growth of active organic films on insulating substrates is driven by the weak van der Waals molecular interactions, whereas interaction with the substrate and presence of metallic electrodes in the vicinity of the contact area affect the film morphology and, hence, the conduction properties of the ultrathin active layer.[3]

On metal surfaces, planar growth of organic molecules is favored by the maximization of the overlap between the π-molecular orbital and the substrate surface charge density. In general, the first hybridized organic layer is expected to be followed by the coherent growth of a planar multilayer film; whenever π-stacking is favored in the molecular crystal, like for planar molecules such as phthalocyanines,[4] perylene derivatives (e.g., PTCDA),[5,6] etc. Apart from the first layer, a π-conjugated molecule of pentacene ($C_{22}H_{14}$) is expected to stand up on metal surfaces, since (i) the growth of the molecular crystal proceeds by stacking of bi-layers, where the molecules are packed in a herringbone structure with almost vertical orientation, and (ii) the low pentacene diffusivity on metal surfaces increases the surface roughness.[7]

The use of supersonic molecular beam epitaxy has been shown to be a viable route to overcome diffusion-limited processes on the growing molecular crystal.[8] This technique allowed the growth of planar films of pentacene on Ag(111) up to ∼50 ML,[9,10] by stacking molecules in a geometry similar to that of (110) pentacene bulk planes, where the long molecular axis lies within the plane.[11,12] As an alternative, an appropriate choice (from both the structural and chemical point of view) of the substrate could force a monolayer geometry mimicking the pentacene (110) bulk planes, thus producing a template for a controlled growth morphology. This route has been effectively pursued on the anisotropic Cu(110) surface, where a planar phase of pentacene was stabilized up to 1−1.5 nm thickness.[13,14]

More recently, the Au(110) surface has been adopted to drive the oriented growth of pentacene films.[15−17] In the submonolayer coverage range, a planar phase with commensurate 3-fold symmetry has been reported, whereas contradictory results were obtained for films of larger thickness. AFM data showed that, after the wetting of the substrate with two-dimensional, 2D, phase of 3-fold symmetry, further molecules aggregate into large 3D stripes with preferred vertical orientation of the molecules.[16] On the contrary, Guaino and co-workers reported STM images of an annealed multilayer π-stacked film, where flat lying molecules are aligned side-by-side, with their long molecular axis oriented along the [001] direction, and form long chains extending in the $[1\bar{1}0]$ substrate direction.[17]

To better investigate this system, we have performed real time measurements of both He Atom Scattering (HAS) and X-ray photoemission spectroscopy (XPS) at the ALOISA branchline (Elettra Synchrotron, Trieste). HAS is ideally suited to study the growth of organic films since it is a non destructive technique, and pentacene films have been reported to be very sensitive to electron irradiation damage.[13] From a general point of view, HAS probes the surface charge corrugation in the reciprocal space like STM does in the direct space, thus yielding fundamental information for the interpretation of both STM images and diffraction measurements with other probes. As a matter of fact, neither STM[18] nor LEED[19] can unambiguously resolve the surface structure when organic molecules are deposited on metals, since STM smears the fast dynamical vibrations of the molecules and LEED has a larger sensitivity to the large Z metal atoms. On the other hand, XPS is well suited to determine the effective amount of molecules deposited on the surface and belonging to the different phases. We have found that pentacene commensurate phases on Au(110) are only formed in the monolayer range. In particular, the (3×6) phase corresponding to the same symmetry reported by Guaino in the

* Corresponding Author: fax: +39-040-226767; e-mail: floreano@tasc.infm.it.

† CNR−INFM Laboratorio Nazionale TASC.

‡ Also at: Department of Physics, University of Ljubljana, Ljubljana, Slovenia.

§ Also at: Jo_ef Stefan Institute, Ljubljana, Slovenia.

|| Also at: Department of Physics, University of Trieste, Trieste, Italy.

10.1021/jp055516p CCC: $33.50
Published on Web 02/17/2006

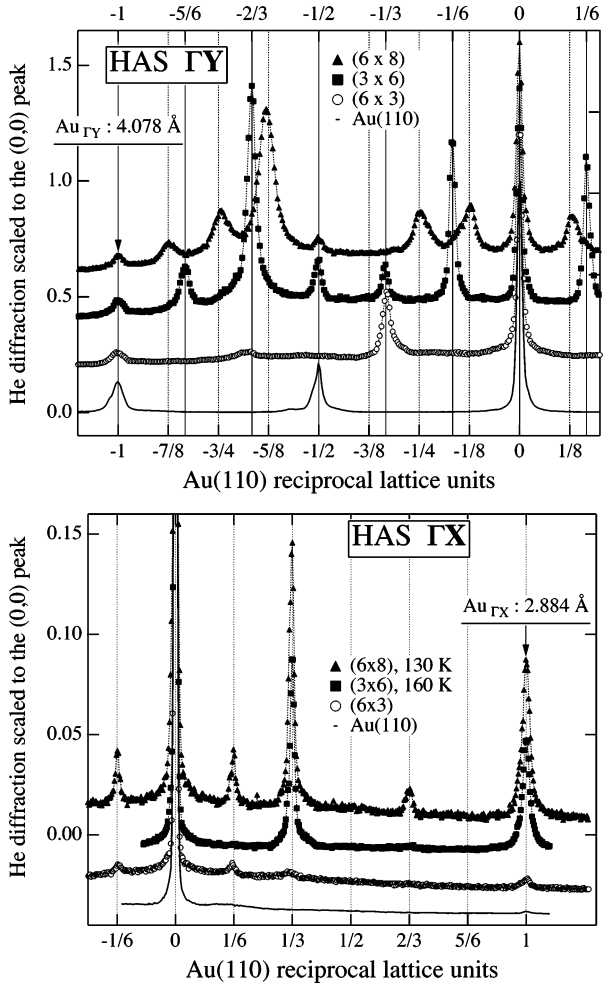

Figure 1. Upper panel: He diffraction patterns along the [001], ΓY, direction collected at RT after deposition at $T_s = 420$ K for the (6 × 8) phase (filled triangles) and $T_s = 470$ K for the (6 × 3) and (3 × 6) phases (open circles and filled squares, respectively). The 2-fold symmetry pattern of the clean missing row reconstructed substrate is also reported at the bottom of the graphic (full line). The diffraction patterns are normalized to their specular reflectivity; a vertical offset has been added for the sake of clarity. The horizontal *x* axis has been normalized to the substrate unit cell along Γ*Y*. As a guide to the eye, fractional peaks of the eighth order are indicated at the bottom *x* axis, while fractional peaks of the sixth order are reported at the top *x* axis. Bottom panel: diffraction patterns of the same phases collected along the [1$\bar{1}$0], Γ*X*, direction. Two patterns (as indicated in the textbox) have been taken at low substrate temperature to reduce the Debye−Waller attenuation. The diffraction patterns are normalized to the specular intensity. The horizontal *x* axis has been normalized to the substrate unit cell along Γ*X*.

multilayer film can be only stabilized in the first molecular layer. Moreover, a novel (6 × 8) equilibrium monolayer phase has been found at a slightly larger coverage.

2. Experiment

Helium diffraction measurements have been taken with the HAS apparatus at the INFM−TASC Laboratory, which is described in detail elsewhere.[20] The HAS apparatus has been equipped with a new hemispherical electron spectrometer (150 mm mean radius) and attached to the ALOISA branchline (130−1300 eV photon energy range) for real time HAS and X-ray photoemission experiments.[21] One-dimensional He diffraction patterns have been taken at a beam energy of 19 meV ($K_{He} \sim 6.1$ Å^{-1}) by polar rotation of the sample. The (1 × 2) diffraction patterns taken on the clean substrate are shown in Figure 1 (full lines) for the two main symmetry directions [001], Γ*Y*, and [1$\bar{1}$0], Γ*X*. The missing row reconstruction yields half-integer diffraction peaks along Γ*Y*, corresponding to a separation of 8.16 Å between the gold troughs.

The pentacene molecules were evaporated from a boron nitride Knudsen cell in a temperature range around 500 K, that corresponds to typical deposition rates of the order of a few monolayers (ML) per hour. We checked routinely for contamination by acquiring XPS spectra in the O 1*s* region at a photon energy of 650 eV. We never observed any trace of O 1*s* on the pentacene covered surfaces, not even 60 h after film deposition. The substrate temperature T_s has been monitored by means of two K-thermocouples spot-welded on a tantalum sheet in contact with the Au(110) sample. Consecutive diffraction patterns have been acquired in real time during pentacene evaporation for different substrate temperatures, as well as real time XPS spectra of the C 1*s* and Au 4*f* core levels have been taken at two photon energies (400 and 650 eV).

3. Results

3.1. Phase Symmetry. Upon pentacene deposition at room temperature (RT) the substrate diffraction pattern rapidly disappears due to the proliferation of pentacene induced defects without yielding any ordered structure. This finding is indicative of a disordered growth, which is in agreement with previous observations.[15−17] Appreciable diffraction features can only be detected upon deposition at a higher substrate temperature. Representative diffraction patterns of the different high-temperature ordered phases are shown in Figure 1 along the two main symmetry directions of the Au(110) substrate.

The highest coverage phase is found to display a previously unobserved (6 × 8) symmetry. This phase corresponds to the saturation coverage at a substrate temperature $T_s = 420$ K. In fact, no change in the diffraction patterns is observed by further pentacene deposition, indicating that no further phases build up beyond the (6 × 8) one at this temperature. In addition, a step-flow growth mode at $T_s \geq 420$ K can be also excluded by comparison with the XPS measurements shown in the next section. At a slightly lower coverage we observed the formation of a (3 × 6) phase, which is the most stable one and corresponds to the saturation coverage at a substrate temperature $T_s = 470$ K. As a consequence, we can exclude the occurrence of a multilayer pentacene film with (3 × 6) symmetry, that was previously reported on the basis of an STM evaluation of the step height difference between adjacent (3 × 6) terraces.[17]

A fainter and broader (6 × 8) diffraction pattern can also be obtained at temperatures as low as $T_s = 370$ K. In this case, continuing deposition slowly leads to an attenuation of the diffraction pattern without any change of the peak position and width. This behavior is characteristic of a Stranski−Krastanov growth, where uncorrelated 3D pentacene clusters grow on top of the first wetting layer. It is important to underline that the (6 × 8) phase can be also obtained by deposition at 420 K on a (3 × 6) phase previously grown at 470 K. In this case, a much longer additional exposure, as compared to deposition on the clean substrate at 420 K, is required; this aspect will be discussed in more detail in the next section together with XPS measurements. For substrate temperatures equal or lower than 370 K, deposition on previously prepared (3 × 6) and (6 × 8) templates simply leads to the attenuation of the diffraction patterns without modifications of their shape, due to 3D (for $370 \leq T_s \leq 420$ K) or disordered (below 370 K) growth. In any case, the (3 × 6) phase is always recovered upon flashing to 470 K the (6 × 8) phase, as well as any higher coverage pentacene film. This

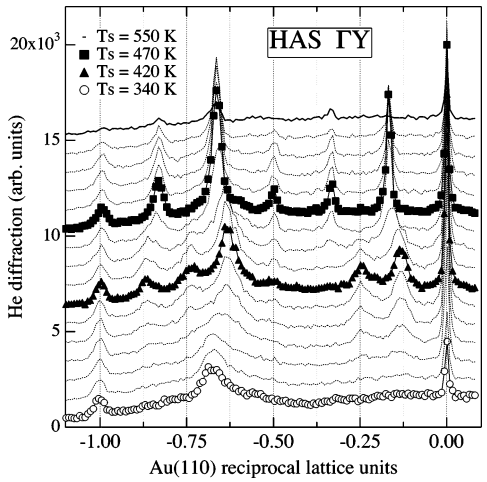

Figure 2. He diffraction patterns collected consecutively during slow surface annealing along the [001] direction. The bottom curve (open circles) is taken just after the deposition of ~2 ML at $T_s = 340$ K. Consecutive scans differs by about 10−15 °C, and they have been displaced vertically by a constant offset for the sake of clarity. The diffraction patterns are to scale, and the overall intensity decrease with increasing temperatures is due to the Debye−Waller attenuation. The horizontal *x* axis has been normalized to the substrate unit cell along Γ*Y*.

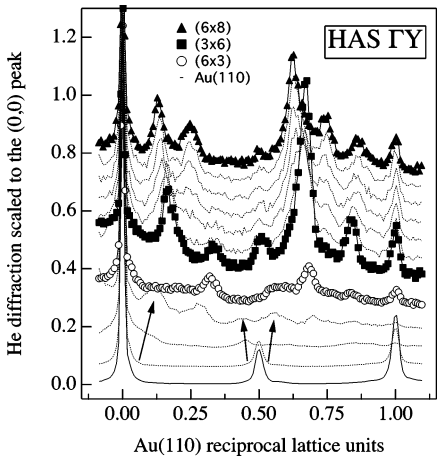

Figure 3. He diffraction patterns collected consecutively along the [001] direction, during pentacene deposition at $T_s = 420$ K. Each scan has been normalized to its specular reflectivity. The diffraction patterns have been vertically shifted by a constant offset for the sake of clarity. The arrows indicate the evolution of the side-peaks at both the specular and half-integer peaks. The horizontal *x* axis has been normalized to the substrate unit cell along Γ*Y*.

is clearly seen in Figure 2, where consecutive HAS patterns have been taken during slow annealing of a ~2 ML film grown at 340 K. As can be seen, pentacene self-organization first leads to the formation of the (6 × 8) phase at 420 K, then residual molecules evaporate leaving a (3 × 6) phase above 470 K.

We have also studied the evolution of the diffraction patterns in the early stage of pentacene deposition. In the substrate temperature range between 420 and 470 K, we clearly observe the splitting of the half integer peaks and the appearance of side-peaks at the specularly reflected (0,0) peak in the early deposition stages, as shown in Figure 3. This observation suggests that the missing row deconstruction is driven by the proliferation of out-of-phase domain walls, which arise from the onset of a correlation among the molecule induced Au defects. The gradual shift of the satellite peaks leads to an intermediate almost 3-fold symmetry along Γ*Y*, like previously observed for the monolayer deposition of sexithiophene.[22] The

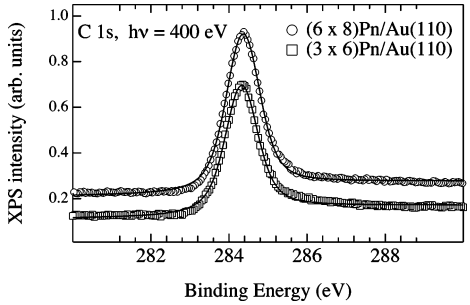

Figure 4. X-ray photoemission spectra of the C 1*s* core level taken for the (6 × 8) and (3 × 6) pentacene phases (open circles and squares, respectively). Spectra taken with a photon energy of 400 eV and an overall energy resolution of 270 meV. A simple fitting to a Voigt function with an integrated background is also shown (full lines). The binding energy scale has been calibrated to that of the Au $4f_{7/2}$ core level peak at 84 eV. The (6 × 8) spectrum has been vertically shifted by 0.1 for the sake of clarity.

formation of a *quasi*-(6 × 3) symmetry can be observed, by stopping the pentacene exposure at the appearance of the 3-fold symmetry ($T_s = 420-470$ K) and cooling the sample to reduce the Debye−Waller attenuation, as shown in Figure 1. It is worth noticing that the fractional peaks of the *quasi*-(6 × 3) pattern display an overall intensity envelope (surface rainbow) quite different with respect to the rainbow of the (3 × 6) and (6 × 8) phases. This large difference among the HAS rainbows indicates a different corrugation of the surface charge density in the pentacene phases, i.e., of the molecular orientation.

We noticed that a very broad diffraction pattern resembling a 3-fold periodicity along ΓY can be also obtained by deposition at 330−340 K (for example, see the bottom curve in Figure 2). In this case, the surface symmetry does not evolve any longer, probably because this temperature range is sufficiently high to allow an initial regular arrangement driven by a substrate reconstruction (thanks to the high mobility of the perturbed Au atoms), but not enough to let the pentacene molecules to self-organize into an ordered overlayer.

3.2. Phase Coverage. The photoemission spectra of the C 1*s* core level corresponding to the two saturation coverage phases are shown in Figure 4. The integrated intensity ratio between the (3 × 6) and (6 × 8) C 1*s* spectra is found to be 8:9 within a precision of 1% (the same ratio is found at both 400 and 650 eV photon energy). No appreciable energy shift is detected between the two peaks. We remark that, while the two phases yield C 1*s* peaks of identical shape, a multicomponent curve is required for an accurate fitting of the broad (almost 1 eV, fwhm) and asymmetric C 1*s* peak. Further pentacene deposition at room temperature or lower leads to a gradual shift of the C 1*s* peak toward larger binding energies, as its intensity increases (3D growth). For a bulk pentacene film obtained by depositing about 10−12 ML at 280 K, we have found a C 1*s* binding energy $E_b = 284.76$ eV, corresponding to a shift $\Delta E_b = +0.38$ eV, with respect to the (3 × 6) and (6 × 8) phases.

To better determine the effective amount of deposited pentacene, we have followed the evolution of the XPS spectra as a function of the pentacene exposure, as shown in Figure 5. At a substrate temperature of 470 K, the C 1*s* signal increases linearly up to a saturation level, corresponding to the formation of the (3 × 6) monolayer phase. A slightly larger saturation level is achieved by deposition at $T_s = 420$ K, where the (6 × 8) monolayer phase is finally established. Most interestingly, the C 1*s* signal is observed to grow linearly up to the intensity level corresponding to the coverage of the (3 × 6) phase. Subsequently the C 1*s* signal grows with a lower rate. A similar

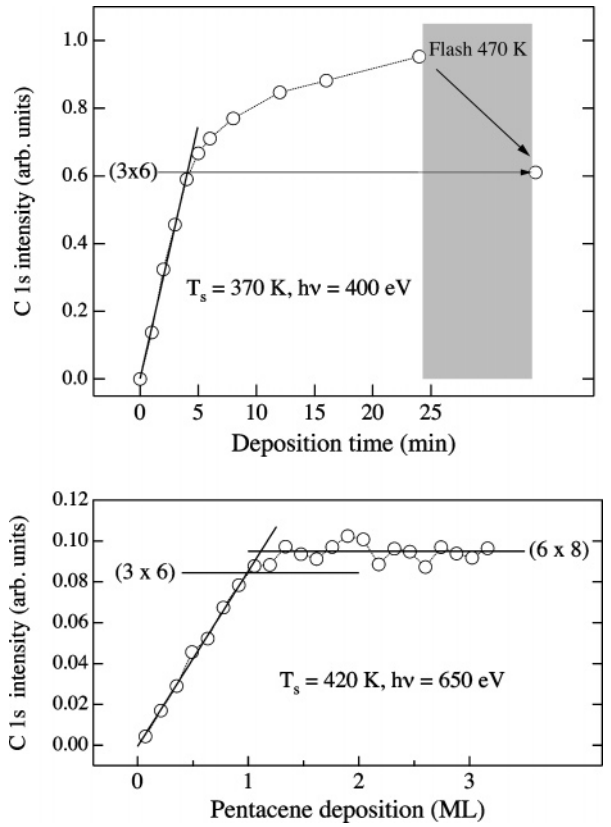

Figure 5. Upper panel: integrated intensity of the C 1*s* XPS spectra taken during deposition at $T_s = 370$ K and with a photon energy of 400 eV. The deposition has been stopped after 24 min. and XPS spectra have been measured after flashing the film to 470 K, yielding a (3 × 6) diffraction patterns. Lower panel: integrated intensity of the C 1*s* spectra taken during deposition at $T_s = 420$ K and with a photon energy of 650 eV. At saturation, a (6 × 8) pattern is detected by HAS. The signal level corresponding to the (3 × 6) phase is also shown. The coverage has been calibrated by conventionally associating the completion of the first organic layer (ML) with the coverage where the C 1*s* signal ends its linear increase, i.e., with the coverage of the most stable (3 × 6) phase.

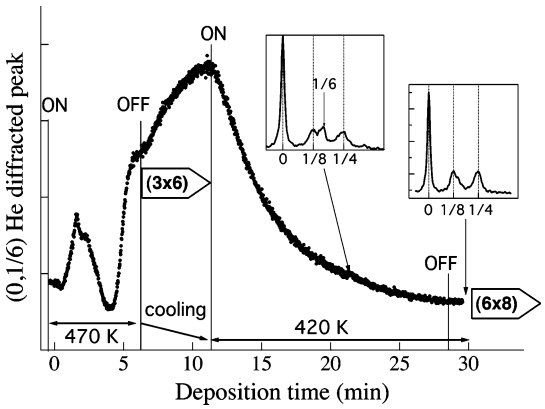

Figure 6. HAS intensity of the (0, 1/6) diffracted peak during deposition at constant rate. The surface is first brought at 470 K, then the shutter is open (label *ON*) for deposition until the (0, 1/6) peak saturates, after about six minutes. At this stage an optimal (3 × 6) phase is formed and the shutter is closed (label *OFF*). Then the surface is cooled to 420 K, correspondingly the (0, 1/6) peak intensity increases due to the Debye−Waller effect. When the surface temperature is stabilized at 420 K the shutter is open again and the peak intensity starts to decrease slowly. After an additional exposure of ∼10 min, we close the shutter and check the diffraction pattern, as reported in the inset graphic at the left. At this stage both the (6 × 8) and (3 × 6) phases coexist. Thus we continue the deposition until the (0, 1/6) intensity decreases to a constant minimum intensity, where the shutter is closed again. At this stage, the HAS pattern only displays a (6 × 8) symmetry phase, as reported in the inset graphic at the right.

behavior is observed at $T_s = 370$ K, where no saturation occurs during growth. The C 1*s* signal grows linearly with the deposition time up to a level corresponding to that of the (3 × 6) phase. Further deposition increases the C 1*s* signal with a decreasing rate. Finally, we observe a decrease of the C 1*s* signal down to the level of the (3 × 6) phase, by annealing the thick film to 470 K.

The linear increase of the C 1*s* signal is associated with the 2D growth of a wetting pentacene layer; its completion corresponds to the coverage of the (3 × 6) phase. As can be seen in Figure 5, the additional pentacene exposure required to form the (6 × 8) phase does not yield a linear increase of the C 1*s* signal any longer. This effect may be due either to the adsorption of the additional molecules on top of the first pentacene layer (where the sticking coefficient might be lower than on the bare substrate), or to the incorporation of the additional molecules in a denser first layer phase. The occurrence of second layer molecules can be excluded on the basis of the absence of any appreciable core level shift or shape difference between the C 1*s* spectra of the two phases (see Figure 4). This result is also confirmed by considering the growth kinetics of the (6 × 8) phase, as obtained by comparing the deposition on the clean substrate with the deposition on a previously prepared (3 × 6) phase. In Figure 6, we report the HAS intensity of the (0, 1/6) diffracted peak (that represents the order parameter of the (3 × 6) phase) and must disappear in the (6 × 8) phase. The deposition at constant rate is shown, starting from the preparation of the (3 × 6) phase at at T_s = 470 K. At the saturation of the (3 × 6) phase, the deposition is stopped. Then the surface is cooled to $T_s = 420$ K, where the deposition is started again. As can be seen, the additional pentacene exposure needed to form the (6 × 8) phase (∼17 min) is remarkably larger than what is required to grow the (3 × 6) phase (∼6 min). Moreover, this additional exposure is larger than the total exposure required to grow the (6 × 8) phase starting from the clean substrate (compare with deposition at $T_s = 420$ K reported in the lower panel of Figure 5). If the (6 × 8) phase was simply given by the condensation of a few molecules on top of the (3 × 6) phase, the total exposure should be roughly independent from the different paths to prepare the (3 × 6) phase underneath.

The facts that (i) the pentacene exposure required to form the (6 × 8) depends on the history of deposition and (ii) the optimal (3 × 6) phase cannot be formed at 420 K, indicate that the (6 × 8) phase is also a monolayer phase with a pentacene packing denser than the (3 × 6) one. The incorporation of additional molecules in the pre-deposited (3 × 6) phase is inhibited by the lower concentration of defects of the (3 × 6) phase grown at 470 K, as compared with that formed at 420 K.

4. Discussion

A summary of the pentacene growth mode on Au(110) is shown in the phase diagram of Figure 7. Concerning the structural evolution of the pentacene film in the submonolayer range, our diffraction measurements are in perfect agreement with the picture drawn by previous STM studies. At low coverage, pentacene molecules are reported to line up into head-to-head chains extending along the [110] direction and inducing a local reconstruction of the Au substrate into (1 × 3) troughs.[17] The *quasi*-(6 × 3) symmetry, that we observe before the formation of the (3 × 6) monolayer phase, has a 17.3 Å long

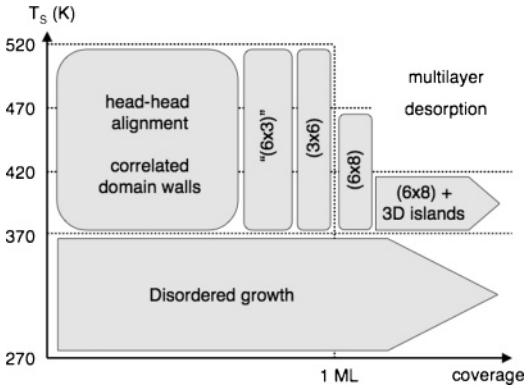

Figure 7. Phase diagram of pentacene films on Au(110). The (6 × 3) phase is quoted since it has not a well defined equilibrium coverage. The completion of the first monolayer is conventionally assigned between the (3 × 6) and (6 × 8) phases. See text for further explanations.

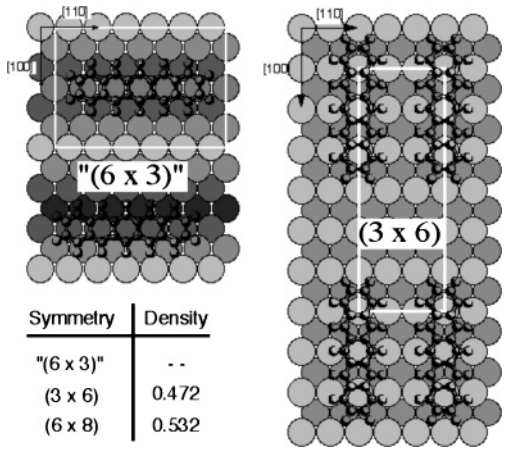

Figure 8. A sketch of the pentacene orientation in the low coverage range is shown in the left panel, where the molecule lies flat within 3-fold troughs. The two possible (1 × 3) reconstructions (shallow and deep troughs) are shown. The relative position of the molecule with respect to the Au atoms is arbitrary. The orientation of pentacene in the (3 × 6) phase is shown in the right panel, after STM pictures of ref 17. The relative position of the molecule with respect to the substrate as well as the substrate reconstruction are arbitrary. The molecular density (in molecules/nm^2) of the different phases is given in the table. The density of the (3 × 6) phase is determined on the basis of the model by Guaino et al.[17] The density is not given for the (6 × 3) symmetry, since it does not correspond to an equilibrium coverage phase. The density of the (6 × 8) phase is determined by the XPS ratio.

side that fits well to the 15−16 Å length of the pentacene molecule.[11,12,23,24] The head-to-head pentacene alignment is also consistent with the observed HAS rainbow along Γ*X* (very faint fractional peaks), that yields a very low corrugation of the surface charge density. This configuration is rather common for adsorbates on the Au(110) surface, since higher order substrate reconstructions along [001] are expected to be energetically very close to the (1 × 2) missing row reconstruction.[25] Submonolayer phases with 3-fold periodicity along the [001] direction have been found for sexithiophene,[18,22] Cu-phthalocyanine[19] and perylene,[26] indeed. The deep troughs made by (1 × 3) units (the least expensive higher order missing row reconstruction[27]) are thought to favor the accommodation of π-conjugated molecules, since they expose (111) microfacets wide enough (∼7 Å) for a coplanar adsorption of the aromatic rings. In fact, recent structural studies of the Cu−Phthalocyanine/Au(110) system challenged this *naive* picture, since a shallow (1 × 3) reconstruction was found beneath a 3-fold periodical arrangement of the molecular layer.[19] A thorough X-ray diffraction study would be required to determine the structural interplay between the pentacene overlayer and the substrate reconstruction.

In the present case, the (6 × 3) phase, with one molecule within the unit cell, does not seem to be an equilibrium homogeneous phase, since a slightly larger (15−20%) amount of molecules deposited above 420 K irreversibly drives the film into a highly ordered and largely stable (3 × 6) symmetry phase. This symmetry corresponds to the phase studied by Guaino and co-workers, who reported pentacene molecules to line up side-by-side with their long molecular axis along the [001] direction and forming widely spaced (24.5 Å) chains that extends along the [1$\bar{1}$0] direction,[17] with one molecule within the unit cell too. The molecules are thus azimuthally rotated by 90° with respect to the (6 × 3) phase. A drawing of the molecular orientation of pentacene with respect to the substrate is shown in Figure 8 for the (6 × 3) and (3 × 6) symmetries. In both cases, the substrate reconstruction and the registry of pentacene with the Au atoms are arbitrary. The preferred orientation with the long molecular axis along the [001] direction is the most stable one also for anthracene on the structurally similar Ag-(110) substrate[28] (lattice spacing of 2.89 Å along [1$\bar{1}$0]), as opposed to the Cu(110) case (lattice spacing of 2.56 Å along [110]), where the pentacene long axis is oriented along the [1$\bar{1}$0] direction.[29,30] Recalling that the aromatic rings within the molecule are spaced by ∼2.45 Å, these observations indicate that the different azimuthal orientations of pentacene can be effectively driven by the matching of the molecule inner structure with the substrate lattice.

The geometry of the (6 × 8) phase, that was never reported before, is much less clear on the basis of the present data. The growth of second layer molecules seems to be excluded since (i) the (6 × 8) C 1*s* XPS spectrum has the same shape of the (3 × 6) one, (ii) the (6 × 8) phase can be formed through different kinetic paths, and (iii) its coverage is only slightly larger than that of the (3 × 6) phase, which has a rather low molecular density of 0.472 molecule nm^{-2} (for comparison several single layer phases more than twice as dense can be obtained on the Au(111) surface[31]). Assuming the constraint to the (6 × 8) phase of being a 2D single layer, its cell dimensions of 17.3 × 32.6 Å^2 are compatible with the presence of up to four pentacene molecules in the cell, as might be obtained by a closer packing of the same pentacene chains participating in the (3 × 6) phase. However, this model must be discarded since its surface density (0.71 molecule nm^{-2}) would yield a 2:3 ratio between the densities of the (3 × 6) and (6 × 8) phases, which is not compatible with the observed 8:9 ratio between the corresponding C 1*s* spectra. The latter ratio would imply the (6 × 8) phase to contain exactly three pentacene molecules within the unit cell (0.532 molecule nm^{-2}). With this constraint, it is not possible to envisage a 2D geometrical model based on a simple displacement of the pentacene chains participating in the (3 × 6) phase and a second azimuthal reorientation has to be considered. As an alternative possibility, a tilting around the long axis of some of the pentacene molecules within the cell might occur, as observed in the widely spaced periodic monolayer phase of pentacene on Au(111).[32]

The few multilayer planar phases, obtained so far on Ag-(111) and Cu(110),[9,13] display a geometry close to that of pentacene (110) bulk planes, where molecules are tilted around their long axis in opposite direction with respect to the layer beneath [herringbone structure in the (100) plane]. In the case of thermal deposition on Cu(110), the density of 0.83 molecule

nm^{-2} of the monolayer phase is close to that of pentacene (110) bulk planes (i.e., 1.05 molecule nm^{-2}), thus second layer molecules can tilt around their long axis and the coupling between the first (flat-parallel) and second (flat-tilted) layers can mimic the herringbone packing of the bulk phase. In the present case, whatever the (6×8) geometry, its density of 0.532 molecule nm^{-2} is much lower than that of pentacene (110) bulk planes, thus second layer molecules cannot be accommodated on the (6×8) and (3×6) templates in a flat lying geometry. On the other hand, the Au(110) substrate structure strongly affects the molecular orientation inhibiting a closer packing of pentacene in the monolayer phases. In any case, it must be emphasized that a close matching between the density of the monolayer phase and that of the pentacene (110) planes appears to be necessary for planar growth but not sufficient. In fact, multilayer films on Au(111) display an upright pentacene orientation and enhanced aggregation into 3D clusters,[33] notwithstanding a planar monolayer phase, with both a density (1.14 molecule nm^{-2}) and a geometry close to that of pentacene (110) bulk planes.[31]

5. Summary

In conclusion, we have shown that two commensurate pentacene phases can be stabilized in the monolayer range on the Au(110) surface. The (3×6) phase, previously reported to be present in multilayer films, is shown to be only formed at high temperature ($\geq$420 K), where second layer molecules do not stick on the surface. A new phase with (6×8) symmetry has been found at a slightly higher coverage. This phase corresponds to the saturation coverage at $T_s = 420$ K and appears to be only formed by first layer molecules. At substrate temperatures $370 \leq T_s \leq 420$ K, pentacene deposition leads to the uncorrelated growth of 3D clusters on a wetting layer both on the clean substrate or on previously prepared commensurate phases. A disordered growth is observed at a substrate temperature lower than 370 K.

Acknowledgment. This project has been co-financed by the University of Trieste and MIUR (PRIN 2003028141).

References and Notes

(1) Dimitrakopoulos, C. D.; Malenfant, P. R. L. *Adv. Mater.* **2002**, *14*, 99.
(2) Dimitrakopoulos, C. D.; B rown, A. R.; Pomp, A. *J. Appl. Phys.* **1996**, *80*, 2501.
(3) Muck, T.; Fritz, J.; Wagner, V. *Appl. Phys. Lett.* **2005**, *86*, 232101.
(4) Hoshino, A.; Takenaka, Y.; Miyaji, H. *Acta Crystallogr. B* **2003**, *59*, 393.
(5) Ogawa, T.; Kuwamoto, K.; Isoda, S.; Kobayashi, T.; Karl, N. *Acta Crystallogr. B* **1999**, *55*, 123.
(6) Krause, B.; Dürr, A. C.; Ritley, K.; Schreiber, F.; Dosch, H.; Smilgies, D. *Phys. Rev. B* **2002**, *66*, 235404.
(7) Ruiz, R.; et al. *Chem. Mater.* 2004, *16*, 4497; and references therein.
(8) Iannotta, S.; et al. *Appl. Phys. Lett.* **2000**, *76*, 1845.
(9) Casalis, L.; Danisman, M. F.; Nickel, B.; Bracco, G.; Toccoli, T.; Iannotta, S.; Scoles, G. *Phys. Rev. Lett.* **2003**, *90*, 206101.
(10) Danisman, M. F.; Casalis, L.; Scoles, G. *Phys. Rev. B* **2005**, *72*, 085404.
(11) Holmes, D.; Kumaraswamy, S.; Matzger, A. H.; Vollhardt, K. P. *Chem. Eur. J.* **1999**, *5*, 3399.
(12) Mattheus, C. C.; Dros, A. B.; Baas, J.; Meetsma, A.; de Boer, J. L.; Palstra, T. T. M. *Acta Crystallogr. C* **2001**, *57*, 939.
(13) Söhnchen, S.; Lukas, S.; Witte, G. *J. Chem. Phys.* **2004**, *121*, 525.
(14) Lukas, S.; Söhnchen, S.; Witte, G.; Wöll, Ch. *Chem. Phys. Chem.* **2004**, *5*, 266.
(15) Menozzi, C.; Corradini, V.; Cavallini, M.; Biscarini, F.; Betti, M. G.; Mariani, C. *Thin Solid Films* **2003**, *428*, 227.
(16) Corradini, V.; Menozzi, C.; Cavallini, M.; Biscarini, F.; Betti, M. G.; Mariani, C. *Surf. Sci.* **2003**, *532*−*535*, 249.
(17) Guaino, Ph.; Carty, D.; Huges, G.; McDonald, O.; Cafolla, A. A. *App. Phys. Lett.* **2004**, *85*, 2777.
(18) Prato, S.; Floreano, L.; Cvetko, D.; De Renzi, V.; Morgante, A.; Modesti, S.; Biscarini, F.; Zamboni, R.; Taliani, C. *J. Phys. Chem. B* **1999**, *103*, 7788.
(19) Cossaro, A.; Cvetko, D.; Bavdek, G.; Floreano, L.; Gotter, R.; Morgante, A.; Evangelista, F.; Ruocco, A. *J. Phys. Chem. B* **2004**, *108*, 14671.
(20) Cvetko, D.; Lausi, A.; Morgante, A.; Tommasini, F.; Prince, K. C.; Sastry, M. *Meas. Sci. Technol.* **1992**, *3*, 997.
(21) A presentation of both the beamline and the branchline can be found at http://www.tasc.infm.it/research/aloisa/scheda.php.
(22) Nardelli, M. B.; Cvetko, D.; De Renzi, V.; Floreano, L.; Gotter, R.; Morgante, A.; Peloi, M.; Tommasini, F.; Danieli, R.; Rossini, S.; Taliani, C.; Zamboni, R. *Phys. Rev. B* **1996**, *53*, 1095.
(23) Endres, R. G.; Fong, C. Y.; Yang, L. H.; Witte, G.; Wöll, Ch. *Comput. Mater. Science* **2004**, *29*, 362.
(24) Lee, K.; Yu, J. *Surf. Sci.* **2005**, *589*, 8.
(25) Bernasconi, M.; Tosatti, E. *Surf. Sci. Rep.* **1993**, *17*, 363; and references therein.
(26) Gross, L.; Seidel, C.; Fuchs, H. *Org. Electron.* **2002**, *3*, 7.
(27) Barth, J. V.; Schuster, R.; Wintterlin, J.; Behm, R. J.; Ertl, G. *Phys. Rev. B* **1995**, *51*, 4402.
(28) Shimooka, T.; Yoshimoto, S.; Wakisaka, M.; Inukai, J.; Itaya, K. *Langmuir* **2001**, *17*, 6380.
(29) Lukas, S.; Witte, G.; Wöll, Ch. *Phys. Rev. Lett.* **2002**, *88*, 028301.
(30) Chen, Q.; McDowall, A. J.; Richardson, N. V. *Langmuir* **2003**, *19*, 10164.
(31) France, C. B.; Schroeder, P. G.; Forsythe, J. C.; Parkinson, B. A. *Langmuir* **2003**, *19*, 1274.
(32) Schroeder, P. G.; France, C. B.; Park, J. B.; Parkinson, B. A. *J. Appl. Phys.* **2002**, *91*, 3010.
(33) Beernink, G.; Strunskus, T.; Witte, G.; Wöll, Ch. *Appl. Phys. Lett.* **2004**, *85*, 398.